Journal Pre-proof

Towards understanding the hole making performance and chip formation mechanism of thermoplastic carbon fibre/polyetherketoneketone (CF/PEKK) composite

Jia Ge, Giuseppe Catalanotti, Brian G. Falzon, John McClelland, Colm Higgins, Yan Jin, Dan Sun

PII: S1359-8368(22)00135-4

DOI: https://doi.org/10.1016/j.compositesb.2022.109752

Reference: JCOMB 109752

To appear in: *Composites Part B*

Received Date: 6 October 2021

Revised Date: 9 February 2022

Accepted Date: 14 February 2022

CRediT authorship contribution statement

Jia Ge: Conceptualization**,** Methodology, Investigation, Writing - Original Draft **Giuseppe Catalanotti:** Supervision, Writing - Review & Editing **Brian Falzon:** Writing - Review & Editing **John McClelland:** Software, Resources, Writing - Review & Editing **Colm Higgins:** Resources, Writing - Review & Editing **Yan Jin:** Supervision, Writing - Review & Editing, Funding acquisition, Project administration **Dan Sun:** Conceptualization, Methodology, Investigation, Writing - Review & Editing, Funding acquisition, Project administration.

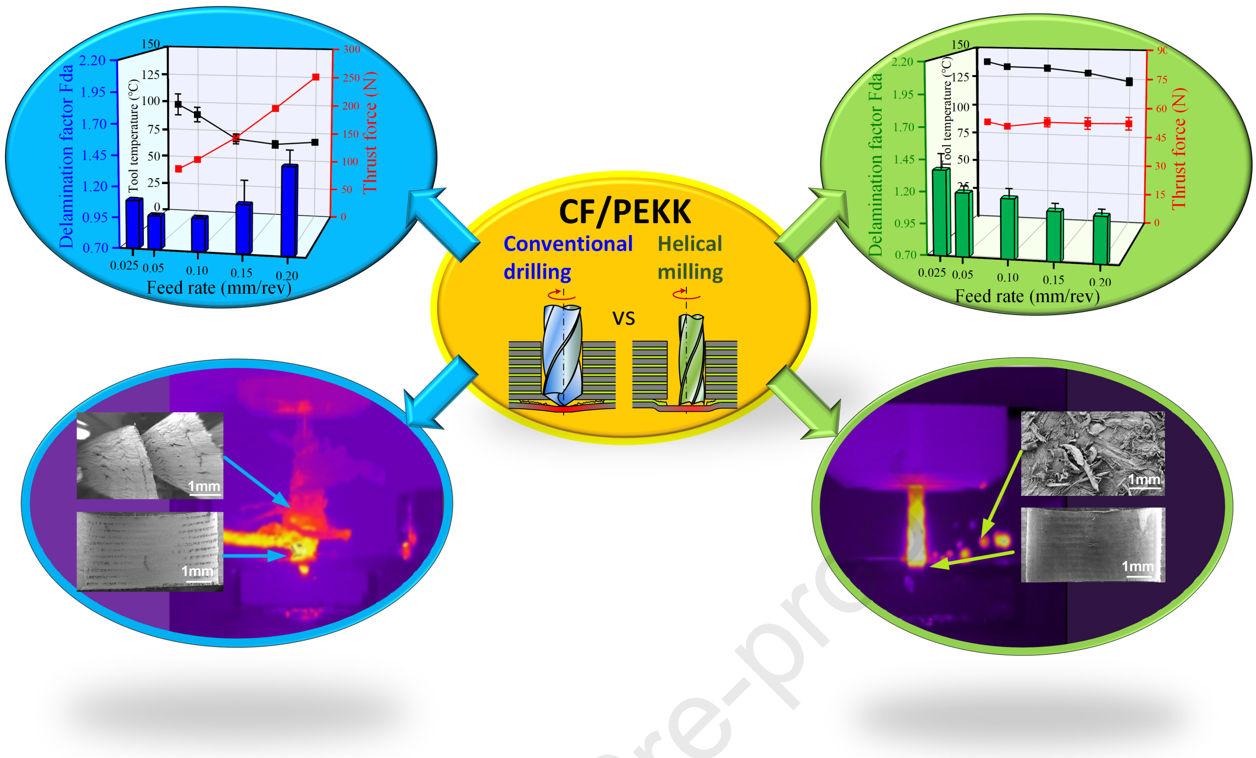
CF/PEKK
Conventional drilling
Helical milling
VS
Delamination factor Fda
Tool temperature (°C)
Thrust force (N)
Feed rate (mm/rev)
1mm

Towards understanding the hole making performance and chip formation mechanism of thermoplastic carbon fibre/polyetherketoneketone (CF/PEKK) composite

Jia Ge[1], Giuseppe Catalanotti[1,2], Brian G. Falzon[1], John McClelland[3], Colm Higgins[3], Yan Jin[1,] Dan Sun[1*]

[1] *School of Mechanical and Aerospace Engineering, Queen's University Belfast, Belfast, BT9 5AH, UK*

**Corresponding author. E-mail address: d.sun@qub.ac.uk*

[2] *Escola de Ciências e Tecnologia, Universidade de Évora, 7000-671 Évora, Portugal*

[3] *Northern Ireland Technology Centre (NITC), Queen's University Belfast, Belfast, BT9 5AH, UK*

Abstract

Here, we report the first study on the hole making performance of thermoplastic carbon fibre/polyetherketoneketone (CF/PEKK). Different hole making methods (conventional drilling vs. helical milling) have been compared and the effect of different feed rates has been investigated. The effect of thermal-mechanical interaction on the resulting hole damage has been elucidated for the first time for carbon fibre reinforced thermoplastics (CFRTPs) hole making. In the material science dimension, advanced material characterization techniques have been deployed to reveal the material removal mechanisms at microscopic scale and unveil the underlying material structural change at a molecular level. Results show that the delamination damage of CF/PEKK is a result of the thermal-mechanical interaction. For conventional drilling, the high machining temperature (at low feed rate < 0.1 mm/rev) has a stronger influence on the delamination damage and the delamination starts to show stronger dependence on the thrust force at high feed rate > 0.1 mm/rev. In contrast, helical milling generates a much higher machining temperature which plays a more predominant role in the associated delamination damage. Microstructural analysis shows that all the hole surfaces feature matrix smearing, as a result of combined in-plane shear stress and high machining temperature. Conventional drilling leads to more severe hole wall microstructural damage (matrix loss and surface cavity) as compared to helical milling. Finally, thermal analysis reveals that the hole making process has led to significantly increased crystallinity in the PEKK matrix as a result of the strain-induced crystallization under the combined effect of shear stress and high temperature.

Keywords: CFRTP, CF/PEKK composite, hole making, delamination damage, polymer crystallinity

1. Introduction

Carbon fibre reinforced plastics (CFRPs) have been intensively deployed in aerospace and automotive industries nowadays, as their high specific strength favours the lightweight design and energy saving requirements of the modern industry. In recent years, there is a surge of interest in the application of novel carbon fibre reinforced thermoplastics (CFRTPs) in the manufacturing sector, as these materials demonstrate several prominent advantages. Compared to the conventional thermosetting CFRPs, CFRTPs require less stringent storage condition and have infinite shelf-life under ambient conditions. Their out-of-autoclave processing can achieve much shorter manufacturing cycle and requires less energy consumption [1]. The thermoplastic nature of the material also endows CFRTP with better recyclability and greater reparability [2], which can contribute greatly to the carbon emission reduction in sustainable manufacturing.

Amongst the available CFRTPs, carbon fibre reinforced polyetherketoneketone composite (CF/PEKK) stands out for its exceptional mechanical properties (tensile strength ~2.4 GPa), strong chemical resistance, high thermal stability (glass transition temperature T_g ~160 ℃) and wide processing window (330 – 380 ℃) [3]. The roadmap for development of thermoplastic composites in Europe, supported by Airbus and a variety of national aerospace consortia (see Fig. 1), suggests that CF/PEKK will be top choice of composite in high end applications such as primary and secondary structural components such as leading edges, floor panels, wing spars and engine pylons in future aircrafts [4–7].

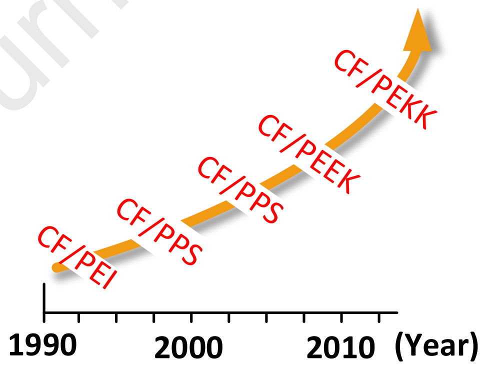

Fig. 1 EU development road map of thermoplastic composites [8]

Like many other CFRTPs, CF/PEKK parts can be manufactured into net shape through compression moulding or assembled by means of welding [9]. However, secondary processing such as mechanical riveting through fastener holes still remains an imperative manufacturing process, particularly in joining of dissimilar materials (e.g. metal/CFRTP joining) and load bearing components [10]. In composite part assembly, conventional drilling (CD) is the most commonly deployed hole making technique due to its great efficiency. Other emerging hole making technology, such as helical milling (HM), has also attracted increasing attention [11]. In HM, the cutter proceeds in both the tangential and the axial directions thus providing combined frontal and peripheral cutting. Compared with CD, reduced burr formation, improved hole geometrical accuracy and smaller cutting force have been reported in HM of aeronautical alloys [12] and thermoset CFRPs [13].

To date, a large body of literature has been dedicated to the study of hole making performance of conventional thermosetting CFRP, covering wide ranging research topics including process optimization [14–16], cutting tool design [17,18], cutting force modelling [19–21] and delamination damage modelling [22–24]. The readers are referred to the review papers [18,25,26] in this field for more information. In comparison, the number of studies concerning hole making performance of CFRTP is very limited. The first study on hole making of CFRTP was conducted by Hocheng and Puw [27] on drilling machinability of CF/acrylonitrile butadiene styrene (CF/ABS). They found that the thrust force in drilling of CF/ABS was proportional to feed rate and highly finished surface ($Ra < 1\mu m$) can be achieved for a wide range of drilling parameters (cutting speed = 1.96 – 50 m/min and feed rate = 30 – 3000 mm/min). In a later study by Hocheng et al. [28], the drilling performance of CF/polyether ether ketone (CF/PEEK) and CF/Polyphenylene sulfide (CF/PPS) was reported. The results showed that thrust force, hole-exit burr and delamination all showed significant increase with increasing feed rate. CF/PEKK composite showed less severe delamination damage due to its high interlaminar fracture toughness. Xu et al. [29] compared the hole making performance of thermoplastic CF/polyimide (PI) and thermosetting CF/epoxy composites under different drilling parameters. The results suggested that CF/PI demonstrated better machinability in terms of lower thrust force/machining temperature and better hole geometrical accuracy. For CF/PI, increasing the cutting speed helped to reduce cylindricity errors, but at the price of higher specific energy consumption. Xu et al. [30] also conducted a full-factorial experimental study to investigate the effect of cutting speed and feed rate on the drilling delamination damage in CF/PEEK and CF/PI. The results showed that delamination damage in both composites can be reduced by increasing the cutting speed or decreasing the feed rate. Lopez-Arraiza et al. [31] compared the performance of three different cutters (reamer, twist drill and drill-end cutter) in hole making of carbon fibre reinforced poly-cyclic butylene terephthalate (CF/pCBT). Results showed that the tool geometry played a crucial role in the resulting hole delamination damage and that the twist drill caused the least delamination damage due to the clearer cutting of the carbon fibre and the pCBT matrix. According to Hocheng et al. [28], the hole making performance of CFRTPs depend on machining parameters, the cutting tools used, as well as the properties of the thermoplastic matrix and the fibre content. To date, no work has been conducted to investigate the hole making performance of high performance CF/PEKK composite and comparative studies on different hole making methods are in scarcity in CFRTP research.

It is known that manufacturing of the thermosetting CFRPs involves a curing process. The resin undergoes a non-reversible chemical reaction and form rigid, covalently boned crosslinks which maintain their rigidity under elevated temperature [32]. In contrast, CFRTPs show typical temperature-dependent property. They soften (lose their mechanical properties) as the temperature approaches its T_g [33] due to the relatively weak Van der Waals' force between their molecular chains. As such, the machining temperature can significantly influence the hole making performance of CFRTPs and should be strictly monitored and controlled. With this in consideration, Xu et al. [29] measured the CF/PI drilling temperature under different feed rates and cutting speeds. Their results suggested that increasing the feed rate can lead to reduced drilling temperature, whereas cutting speed did not have any significant effect. In another study by Xu et al. [30] , the CF/PEEK drilling temperature was measured and results showed that the high machining temperature can soften the matrix and the highly ductile PEKK matrix was recast on to the hole wall, generating the distinct matrix smearing. Similar matrix smearing phenomena were also reported by Hocheng and Puw [27], Ferreira et al. [34] and Kim et al. [35] in drilling of carbon fibre reinforced acrylonitrile butadiene styrene (CF/ABS) and CF/PPS. Although above researchers have studied the machining temperature in hole making of several CFRTPs, they failed to elucidate the impact of high machining temperature on the resulting hole damage formation (especially delamination and hole microstructural damage) and the associated material removal mechanisms.

Recently, several researchers studied the chip formation in drilling of CFRTPs with the aim of establishing the associated material removal mechanisms. Hocheng and Puw [27] compared chips produced from drilling of thermoplastic CF/ABS and thermoset CF/epoxy composites. It was found that CF/ABS featured long continuous chips, which was associated with the better ductility of the thermoplastic matrix and the considerable plastic deformation it experienced during the machining process. In contrast, fragmented chips were produced in drilling of CF/epoxy, indicating the material removal was by means of brittle fracture. In their later work, Hocheng et al. [28] reported that the extent of plasticity in chip formation and the chip length were dependent on the level of fibre content and the deformation behaviour of the matrix. Ahmad et al. [36] and Xu et al. [30] found that the elongated CFRTP chips adhered to the drill bit main cutting edge, which led to severe tool clogging, deteriorated tool cutting performance and accelerated tool wear [36]. So far, no work has been done to investigate the chip microstructure and the associated material removal mechanism of CF/PEKK. The polymer chains within CFRTP matrix will be highly mobile when subjected strong mechanical shearing and high temperature during the hole making process, there has been no study dedicated to understanding the microstructural evolution of machined CFRTP at a molecular level.

In this paper, the hole making performance of advanced thermoplastic CF/PEKK composite is reported for the first time. The effect of different hole making methods (CD and HM) and feed rates on the resulting delamination and hole wall microstructural damage will be discussed, considering the thermal-mechanical interaction arise from the hole making process. The microstructure of the formed chips will be analysed in detail to reveal the fundamental material removal mechanism. In addition, thermal analysis will be carried out for the chips to elucidate the material molecular structural evolution during the machining process. This study will not only reveal the fundamental material science involved in the hole making process, but also provide a parametric and methodological guidance for assembly of load-bearing aircraft parts involving CFRTP components (such as composite-metal stacked structures in frames and wings) [37,38].

2. Experiment setup

2.1. Materials

CF/PEKK (3 mm thick, fibre content 66 wt%) laminates consisting of 22 plies of unidirectional prepregs with a stacking sequence of $[0/90]_{11}$ were manufactured by consolidation method [39] following recommended protocol. The thermoplastic PEKK matrix has a T_g of 160 ℃ and a melting temperature (T_m) of 337 ℃. The coupons for hole making experiment measures 120 mm × 120 mm × 3 mm. Twist drill bit for CD (namely AT Drill) and end milling cutter for HM (namely AT Mill), were supplied by Changzhou Aitefasi Tools Co., Ltd. Changzhou, China. More details of the cutting tools can be found in Table 1.

Table 1 Details of the cutting tools used in this study

Tool abbreviation	Tool name	Image	Diameter (mm)	Flute number	Point angle (°)	Helix Angle (°)
AT Drill	Aitefasi 3D drill bit (TiAlN coated)	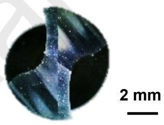	6	2	104	30
AT Mill	Aitefasi standard square end mill (TiAlN coated)	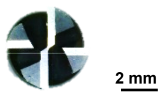	4	4	-	30

2.2. Hole making experiments

Both CD and HM experiments were conducted under dry condition at room temperature. Since axial feed rate is a key parameter in relation to hole delamination formation due to Mode-I opening fracture, five different levels of feed rates (F = 0.025, 0.05, 0.10, 0.15, 0.2 mm/rev) were selected for CD and HM. A cutting speed of V_c =50 m/min was selected to avoid generation of excessive heat and thermal damage of the matrix [40,41]. A tangential feed 0.04 mm/tooth was selected for HM based on previous research [40]. All machining parameters were selected based on the published literature [10,30,41] and per tool manufacturers' recommendation. Both CD and HM were carried out on a Deckle FP3A 3 axis Computer Numerical Control (CNC) machine, which is equipped with an in-house chip extraction system to comply with health and safety regulations. Fig. 2 illustrates the details of the experiment setup. A 3 mm thick steel plate with 10 mm diameter pre-drilled holes was placed on the CFRTP drill-exit side, to ensure consistent supporting stiffness for each hole made [42]. During the hole making process, the thrust force was recorded by a Kistler 9272 4 component dynamometer with a 5070A charge amplifier and a 5697 data acquisition Unit. A thermal camera (FLIR A6751, temperature range: -20 to 350 ℃, frame frequency:125 Hz) was used for real time temperature measurement. The camera calibration and temperature measurement procedures were in accordance with ASTM E1933-14. The image of the cutting tool tip emerging from the hole-exit was captured by the thermal camera and a region of interest (ROI) was selected on the software to calculate the average tool tip temperature, see Appendix Fig. A.1. Three holes were produced and inspected under each set of parameters for repeatability. The cutting tools were replaced after making every three holes to eliminate the effect of tool wear.

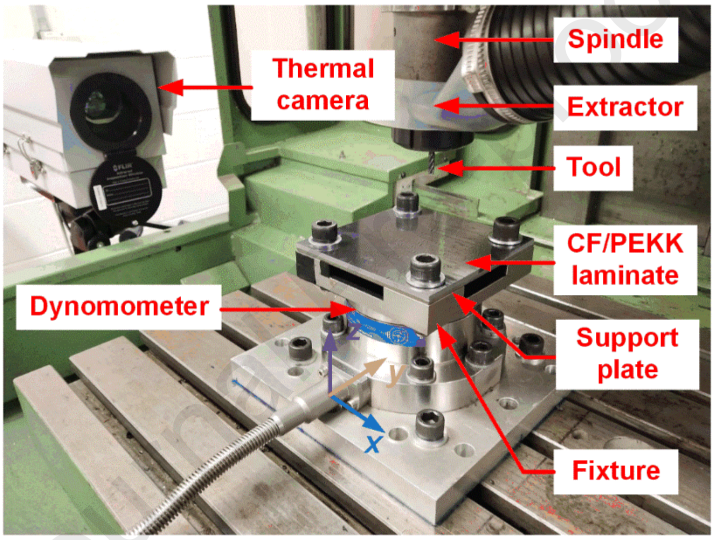

Fig. 2 Image showing the setup of the hole making platform

2.3. Hole quality evaluation

The hole-exit delamination was imaged by Alicona infinite focus G5 microscope (Bruker, UK, 2.5X magnification). The exit delamination (Fig. 3 grey area) can be quantified by the delamination factor F_{da} [43], which can be calculated following Eq. 1-3:

$$F_{da} = \alpha \frac{D_{max}}{D_{nom}} + \beta \frac{A_{max}}{A_{nom}} \quad (1)$$

$$\beta = \frac{A_{dam}}{A_{max} - A_{nom}} \quad (2)$$

$$\alpha = 1 - \beta \quad (3)$$

where D_{max} is the maximum diameter of damaged area, D_{nom} is the nominal diameter of the hole, A_{max} is the area related to the maximum diameter of the delaminated zone (D_{max}), A_{nom} is the nominal hole area and A_{dam} is the damaged area. The delamination factor was calculated through image analysis using MATLAB R2019b software.

The hole wall microstructures and chip morphology were inspected by Scanning Electron Microscopes (SEMs) FlexSEM 1000 (Hitachi Ltd., Japan) under an acceleration voltage of 5 kV. The samples were sputter-coated with gold before SEM observation.

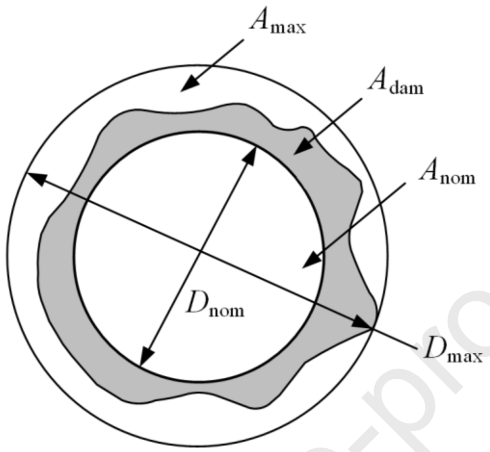

Fig. 3 Schematic of hole-exit delamination

2.4. Thermal analysis

The thermal properties of the CF/PEKK samples were measured using a thermogravimetric analysis (TGA) and differential scanning calorimetry (DSC) thermal analysis system (TGA/DSC2, Switzerland) under a N2 atmosphere in a temperature rage 30 to 550 ℃ and a heating rate of 10 ℃/min.
The crystallinity χ_c of the samples is calculated following Eq. 4 [44]:

$$\chi_c = \frac{\Delta H_m - \Delta H_{cc}}{\Delta H_{100\%}(1 - W_f)} \times 100\% \quad (4)$$

Where ΔH_m is the melting enthalpy, ΔH_{cc} is the cold crystallization enthalpy, $\Delta H_{100\%}$ = 130 J/g is the melting enthalpy of the theoretical 100% crystalline PEKK [45] and $W_f = 66\%$ is the fibre weight fraction in the CF/PEKK composite.

3. Results and discussion

3.1. Thrust force

In hole making of CF/PEKK, thrust force (also known as axial force) corresponds to the level of load exerted on the workpiece by the cutting tool. The thrust force is thought to be directly related to the hole-exit delamination damage caused by Model-I opening fracture, particularly in thermosetting CFRP [46]. The typical force signals in hole making of CF/PEKK are shown in Fig. 4. The thrust force signals for both CD and HM feature three phases, namely, cutting in, stable cutting and cutting out phases. The thrust force measured during the stable cutting phase is representative of the force exerted on the workpiece, therefore the average thrust force of the stable cutting phase was used for further analysis.

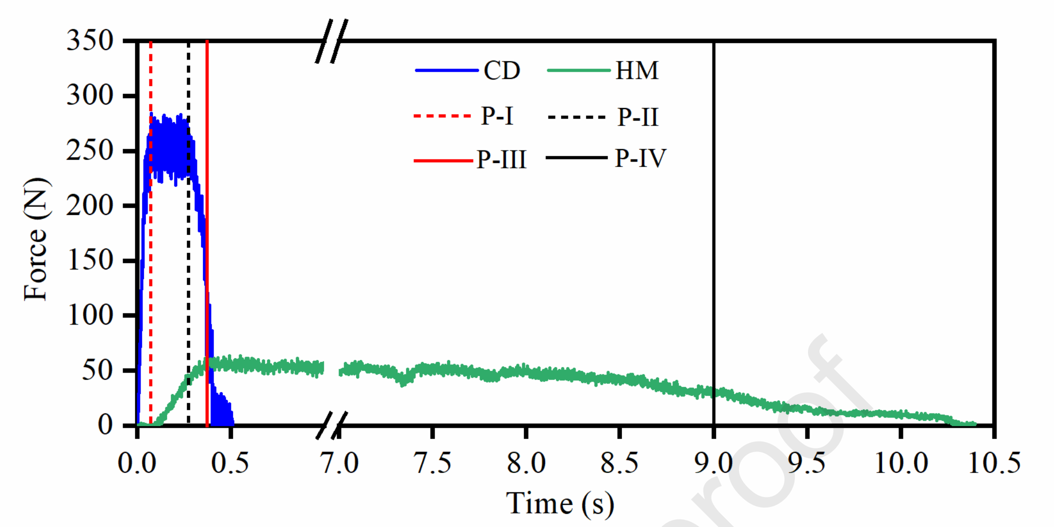

Fig. 4 Representative thrust force signal in CD and HM of CF/PEKK with feed rate F= 0.2 mm/rev. (P-I and P-II depict the starting and ending of the CD stable cutting phase; P-III and P-IV depict the starting and ending of the HM stable cutting phase)

The average stable cutting phase thrust force generated under different feed rates is shown in Fig. 5. HM generated a consistently low thrust force (~ 50 N), which is independent of the feed rate used. Under CD however, the measured thrust forces are significantly higher than that of HM and shows a clear increasing trend with the feed rate.

The difference in thrust force seen in CD and HM can be attributed to the distinctly different material removal mechanisms involved in the two processes. For CD, the cutting speed near the borehole centre approaches zero. The material removal is achieved by extrusion in the axial direction rather than cutting [13], which induces a much higher axial thrust force. For HM, a large portion of material removal is achieved by the peripheral cutting edge as the tool travels along its helical tool path. As a result, less force is exerted in the axial direction.

It can be seen from Fig. 5 that increasing feed rate from 0.025 mm/rev to 0.2 mm/rev has led to ~ 224% increase in thrust force for CD. The drastic increase can be attributed the thicker material removed per tool revolution under the higher feed rate, as shown in Appendix C Fig.C.1. This creates more resistance for tool progression, as greater work is required to achieve deformation/removal of thicker material [19]. For CD, the thrust force showed a quasi-linear correlation with the feed rate, such linear correlation is similar to that reported by Guo et al. [19] in their thrust force models for CD of CF/epoxy composite. The slight deviation from the linearity at lower feed rates ($F \leq 0.05$ mm/rev) may be attributed to the tool clogging (see Fig. 5 insets). When tool clogging occurs, extra force is required to evacuate the stuck chips, and this is added onto the thrust force measured in the axial direction. Tool clogging has also been reported by Ahmad et al. [36] and Xu et al. [30] in their study on drilling of CF/PEEK. Such phenomenon is unique to drilling of CFRTP (not reported in thermosetting CFRP drilling) and should be considered for thrust force modelling in future studies.

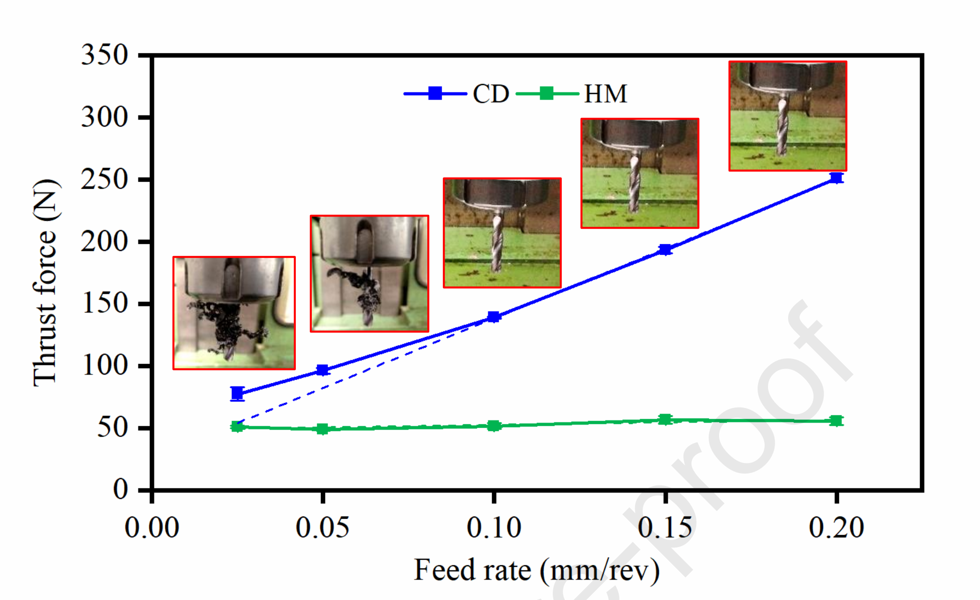

Fig. 5 Effect of feed rate on the thrust force under different hole making conditions (insets: evidence of tool clogging by chips on drill bits)

3.2. Tool temperature

The heat generated during the hole making process is primarily due to the shear deformation of CF/PEKK and the friction between the cutting tool and the workpiece [47]. The accumulated heat is then distributed to the chips, the workpiece and the cutting tool. According to previous experimental and numerical simulation studies by Thirukkumaran et al. [48], the workpiece temperature follows a quasi-linear increasing trend with cutting tool temperature. Given the workpiece hole-exit temperature cannot be measured directly with our existing experimental setup, hole-exit tool temperature was used to inform the machining temperature. The tool temperature under different hole making methods and feed rates is shown in Fig. 6. In general, the tool temperature decreases with increasing feed rates for both CD and HM. For CD, the tool temperature decreased from 98.03℃ to 68.20℃ (a 30.43% reduction) as the feed rate increased from 0.025mm/rev to 0.1 mm/rev. The tool temperature stabilized at ~ 70 ℃ for feed rate > 0.1 mm/rev. In contrast, the tool temperature recorded for HM is much higher for all the feed rates used. The highest HM tool temperature (137.9℃) was recorded at F = 0.025mm/rev, which gradually decreased to 123.15℃ at F = 0.2 mm/rev, marking a 10.70% overall reduction.

For both CD and HM, the lower tool temperature recorded at a higher feed rate can be attributed to the reduced tool-workpiece contact time (i.e., tool engagement time, see Appendix Table B.1). It is clear that the tool engagement time decreases with increasing feed rate and shorter tool engagement time creates less thermal energy accumulation during the machining process. The considerably longer tool engagement time in HM (see Appendix B Table B.1) is accountable for its much higher tool temperature.

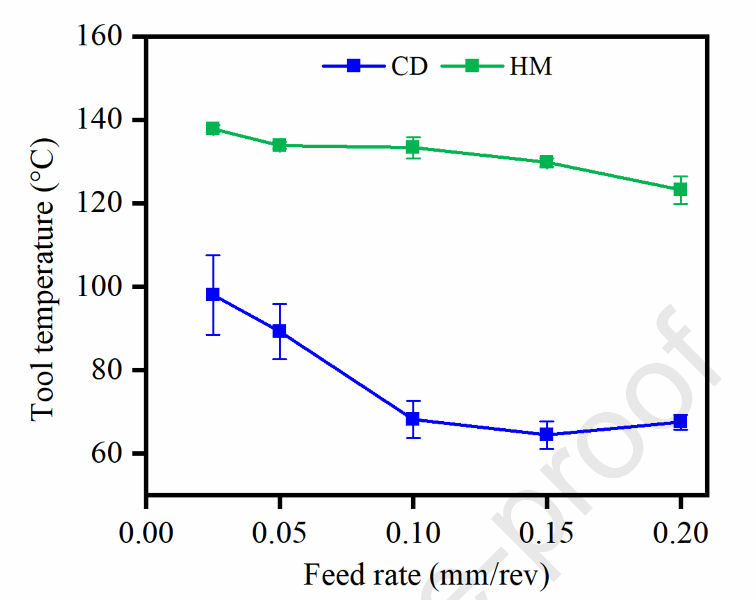

Fig. 6 Tool temperature of CD and HM against feed rate

3.3. Assessment of delamination damage

Delamination, a commonly seen defect at the CFRP hole entry and hole exit, accounts for ~ 60% of composite laminates rejection during assembly [49]. Hole delamination reduces the assembly tolerance and compromises the component's reliability under fatigue loads [46], and therefore should be strictly monitored/controlled during the hole making process. Table 2 shows the binary images of delamination damage produced under different hole making conditions. Although the literature suggests HM induces less hole delamination in hole making of thermosetting CFRP [50], our results show that the extent of hole delamination under different hole making condition is actually feed rate dependent. Under low feed rate, the delamination seen for HM is more severe than CD.

The variation of delamination factor against the feed rate is depicted in Fig. 7. The corresponding tool temperature and the thrust force was also included in the plots. For CD, the initial declining F_{da} ($F < 0.1$ mm/rev) correlates well with the declining tool temperature. Under a lower feed rate ($F < 0.1$ mm/rev), the machining temperature plays a more predominant role in the delamination damage, as the much higher machining temperature under such condition can lead to significant loss of stiffness of the CF/PEKK ply which makes it more prone to delaminate. At higher feed rate, the machining temperature decreased significantly and the drastically increased thrust force would take over its influence on the delamination damage. This is reflected by the increased F_{da} with increasing thrust force for $F > 0.1$ mm/rev.

Table 2 Binary images of hole exit delamination under different hole making conditions

Feed rate (mm/rev)	0.025	0.05	0.1	0.15	0.2
CD	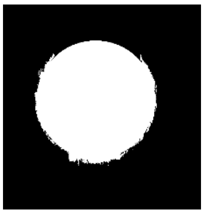	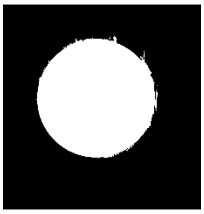	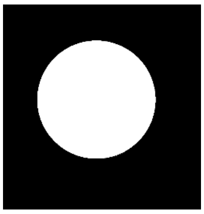		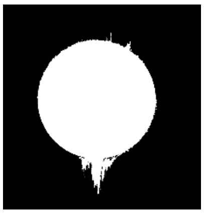
HM	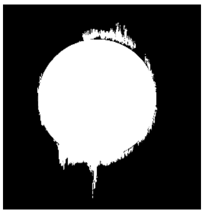	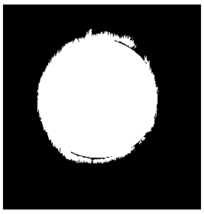	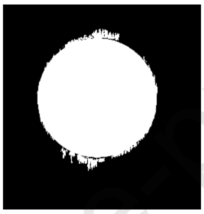	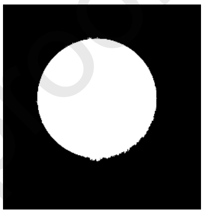	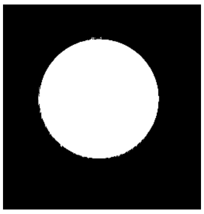

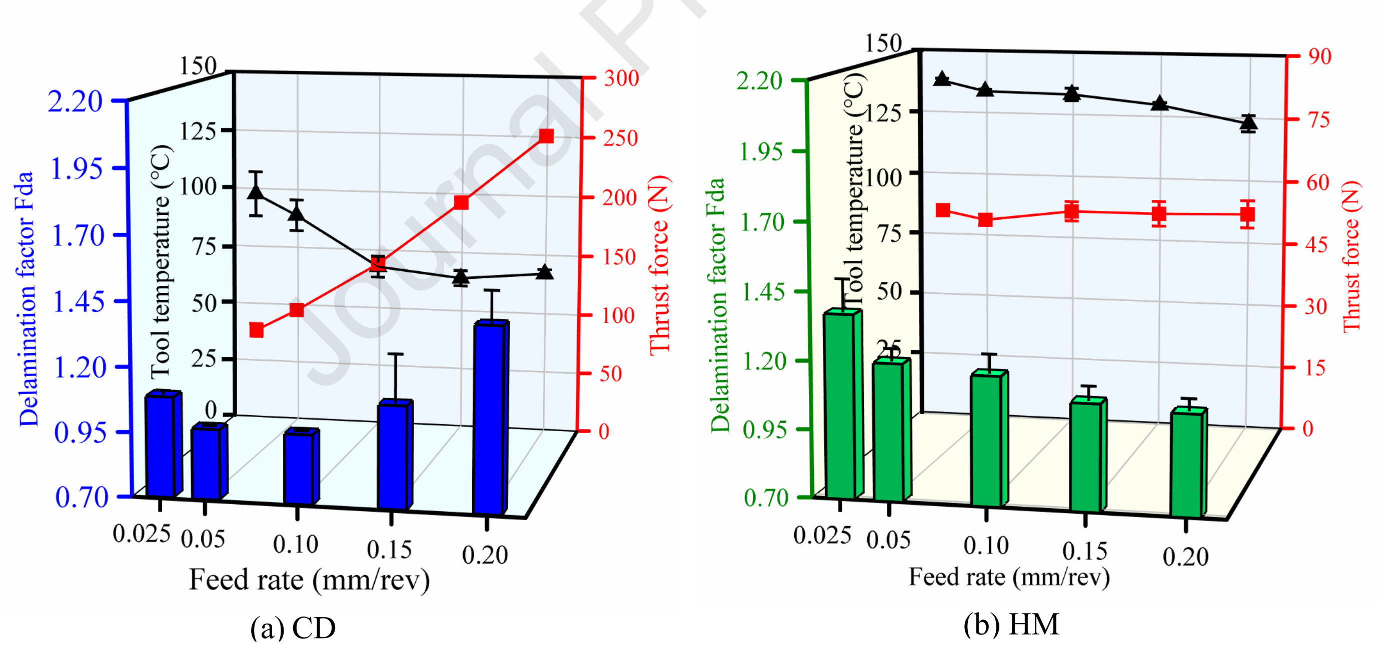

Fig. 7 Delamination factor Fda against feed rate (front bar chart) and variation of tool temperature and thrust force against feed rate (back line chart) for (a) CD and (b) HM

For HM, the thrust force is independent of feed rate and remained at a constant low level (50 N). At low feed rate (0.025 mm/rev), the tool temperature approaches the T_g of PEKK. The gradual declining trend of tool temperature also correlates well with the decreasing F_{da}, implying the influence of tool temperature on the HM delamination

The finding of this study is in contrast to the reports [25,46,51] on thermosetting CFRP, where thrust force is considered the sole factor determining the delamination damage. In thermosetting CFRP, hole-exit delamination is mainly caused by mode I opening fracture as the cutting tool approaches the hole exit and the resulting delamination factor increases with thrust force [18,25,26]. For CF/PEKK however, the elevated temperature caused by the machining process also plays a significant role in the resulting delamination. Given the thermoplastic nature of the PEKK matrix, high machining temperature (approaching T_g) can result in softened matrix [52] and weakened matrix support/encapsulation around the fibre bundles, which contribute to the more severe delamination damage.

3.4. Hole wall microstructure

Microstructural damage such as fibre breakage, matrix loss and debonding can occur during hole making of CFRP. The typical hole wall surface SEM images produced under different hole making conditions is shown in Fig. 8 and Fig. 9.

For CD, low feed rate (F = 0.025 mm/rev) resulted in relatively smooth hole wall surface finish, with negligible matrix loss, see Fig. 8 (a1). Increasing feed rate has led to more severe matrix loss and surface cavity as shown in Fig. 8 (b1) and (c1). The matrix loss and surface cavity typically take place at the obtuse fibre orientation where the material was removed by bending fracture [53]. The cracks and tears caused by the bending stress can be easily transmitted to the hole wall subsurface, resulting in distorted pits when the chip was separated from the workpiece [53]. As can be seen in Fig. 8 (a2-c2) (a3-c3), for both 0° and 90° fibre orientation, the extent of hole wall damage increases with increasing feed rate. The hole wall produced under low feed rate (F=0.025 mm/rev) mainly features matrix smearing, where the fibre is well covered by the thermoplastic PEKK matrix. When the feed rate is increased from 0.025 mm/rev to 0.2 mm/rev, more severe fibre debonding and breakage are evident on the hole surface.

The hole wall microstructure under HM condition is significantly different from that of CD, see Fig. 9. No significant surface matrix loss / cavity has been observed. This may be because the much lower cutting force of HM minimized the fracture and tears produced by the bending stress. The feed rate did not have significant impact on the resulting hole microstructure. For all the feed rates under investigation, 0° ply features long lip-like matrix smearing, whereas 90° ply shows blotchy matrix smearing. This is in contrast to the more even matrix smearing seen on the CD hole wall. The difference can be attributed to the disparate cutting behaviour of HM and CD: the cutting edges of drill bit is in constant contact with the hole wall surface and this can facilitate the evenly smeared PEKK matrix against the hole wall. For HM, the peripheral cutting edges of milling cutter is in intermittent contact with hole wall, which causes more localized matrix smearing. The much higher machining temperature (approaching PEKK T_g) under HM may also lead to reduced matrix viscosity, and hence different matrix smearing behaviour.

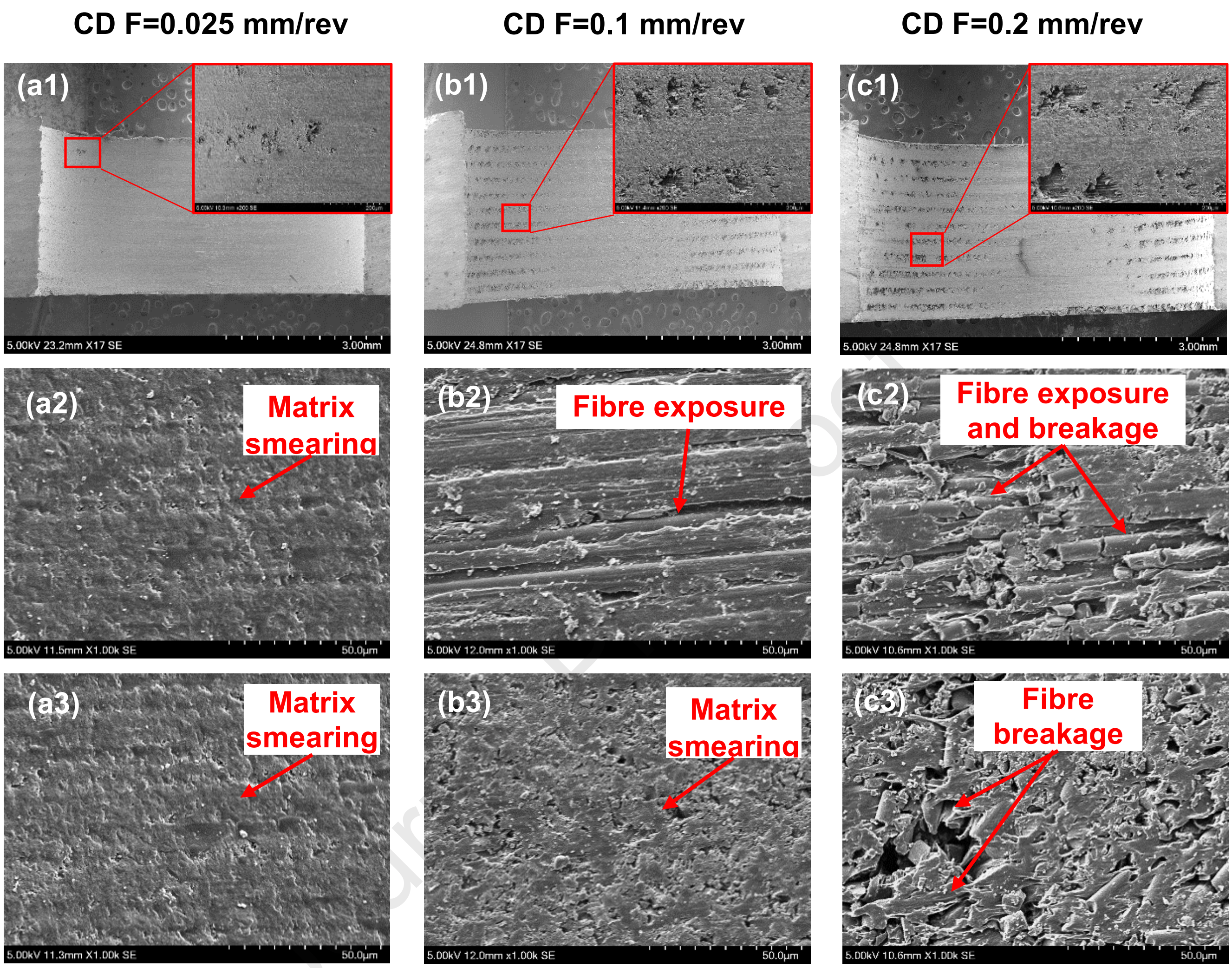

Fig. 8 (a1-c1) Low and high magnification SEM images showing hole wall microstructures produced by CD under different feed rates; (a2-c2) high magnification SEM images showing damage on 0° ply; (a3-c3) high magnification SEM images showing damage on 90° ply.

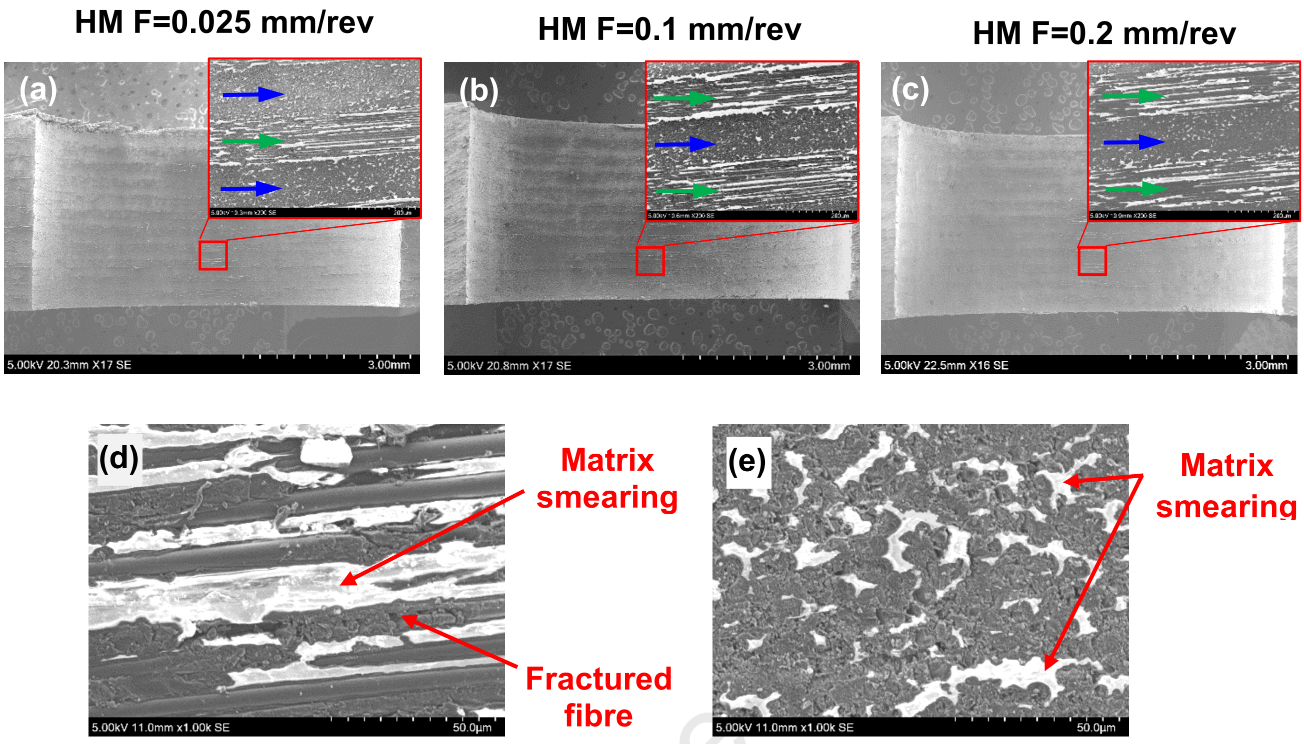

Fig. 9 (a-c) Low and high magnification SEM images showing hole wall microstructure produced by HM under different feed rates (Green arrow: 0° ply, blue arrow: 90° ply); Representative SEM images showing HM hole wall microstructure of (d) 0° ply and (e) 90° ply.

3.5. Chip analysis

3.5.1 Chip morphology

Table 3 shows the optical images of the chips collected from different hole making conditions. In general, chips produced by CD are continuous and ribbon-like, similar to chips produced from drilling of CF/ABS [27] and CF/PEEK [30]. In contrast, chips produced from HM are finer and powder-like. This distinct difference in chip morphology can be attributed to the different material removal mechanisms: CD is a continuous cutting process where the main cutting edge of the drill bit is in continuous contact with the workpiece and the chip flows continuously along the flute after leaving the cutting edge [54]. HM on the other hand, is an intermittent cutting process where the material removal is achieved by the periodic contact between peripheral cutting edge and the workpiece [55].

For CD, extremely long continuous chips were produced at low feed rates (F = 0.025 mm/rev and F = 0.05 mm/rev), which has led to severe tool clogging, (also see Fig. 5). The length of the chips generally decreased with increasing feed rate, as the chips are prone to fracture under greater thrust force. The microstructure of the chips was further analysed by SEM and the results are presented in Fig. 10. It can be seen that for CD under low feed rate (F = 0.025 mm/rev), the chips show a folded morphology. This is because the extremely long chips tend to congest in the flute of the drill bit, impeding their evacuation. In addition, the chips produced under low feed rate are thinner (See Appendix C Fig. C.1) and easily deformed (compressed) when being pushed out of the flute. The spiral CD chip morphology produced under high feed rate (F = 0.2 mm/rev) resembles metal chips produced by CD [56,57]. Such morphology is in contrast to the powdery chips produced from brittle CF/epoxy composite under the similar CD process [30,58,59]. This is mainly due to the excellent ductility of the PEKK matrix (~ 50.0% failure strain) [60], where the thermoset epoxy matrix has a much lower ductility (1.5 - 8.0% failure strain) [60]. For HM, finer and more fragmented chips were evident, see Fig. 10 (c) and (d). Higher feed rates tend to produce slightly thicker chips, as the volume of material removed per tooth increases with the feed rate [13].

Table 3 Morphology of chips produced in hole making of thermoplastic CF/PEKK composite

Feed rate (mm/rev)	0.025	0.05	0.1	0.15	0.2
CD					
HM	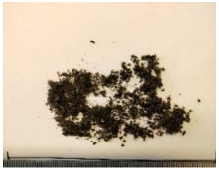	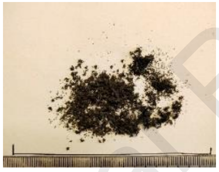			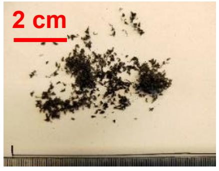

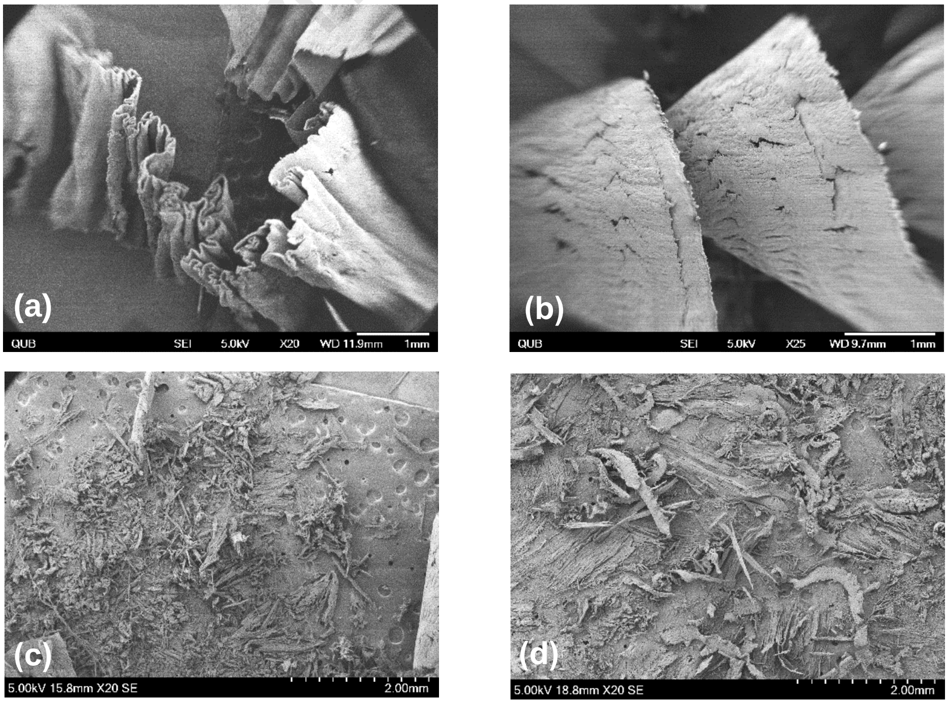

Fig. 10 SEM images of chips produced by (a) CD at F=0.025 mm/rev, (b) CD at F=0.2 mm/rev (c) HM at F=0.025 mm/rev (d) HM at F=0.2 mm/rev

3.5.2 Chip thermal properties

To evaluate the potential impact of the hole making process on the machined composite molecular structure, thermal analysis was carried out for the machined chips using DSC technique, see Fig. 11. The corresponding material thermal parameters obtained from DSC analysis were summarized in Table 4. From Table 4, it can be seen that the crystallinity data χ_c follows the trend CD > HM > control, with CD under F = 0.2mm/rev giving the highest χ_c (28.35%), representing > 300% increase against the control (unmachined CF/PEKK).

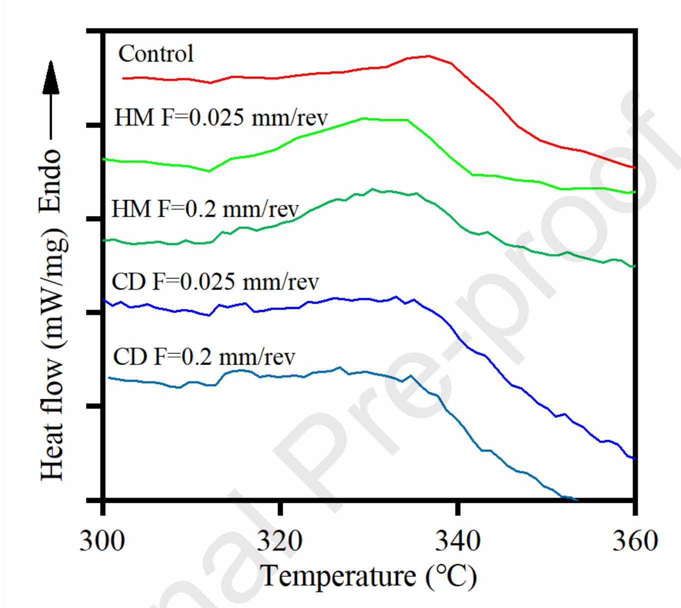

Fig. 11 DSC results of raw material and chips produced under different hole making conditions

Table 4 Crystallinity values of unmachined CF/PEKK and chips produced under different hole making conditions

Hole making method	Feed rate (mm/rev)	ΔH_m (J /g)	ΔH_{cc} (J /g)	χ_c (%)	% increase
Control	-	3.183	-	7.20	-
CD	0.025	9.739	-	22.03	205.96
CD	0.1	12.53	-	23.76	293.65
CD	0.2	12.82	-	28.35	302.76
HM	0.025	6.496	-	14.70	104.08
HM	0.1	6.759	-	15.29	112.34
HM	0.2	6.624	-	14.98	108.10

The increase in crystallinity seen in the machined chips can be attributed to the shear induced crystallization in the thermoplastic PEKK matrix [61]. Shear induced crystallization has been previously reported for thermoplastic polymers such as uniaxially stretched PEEK [61] and powder reinforced thermoplastic nanocomposites (such as boron nitride reinforced polyethylene [62] and graphene reinforced polypropylene [63]) subjected to tension. However, this is the first time such phenomenon was discovered for machined CFRTP. During machining, the tool cutting edge exerts a significant in-plane shear stress on both the hole wall and the adjacent chip. PEKK is a semi-crystalline polymer consisting of both crystalline and amorphous regions. Under the shear action, randomly arranged molecular chains within the PEKK amorphous region will be stretched and re-aligned along the shear direction, forming more orderly arranged crystalline region, as illustrated by Fig. 12.

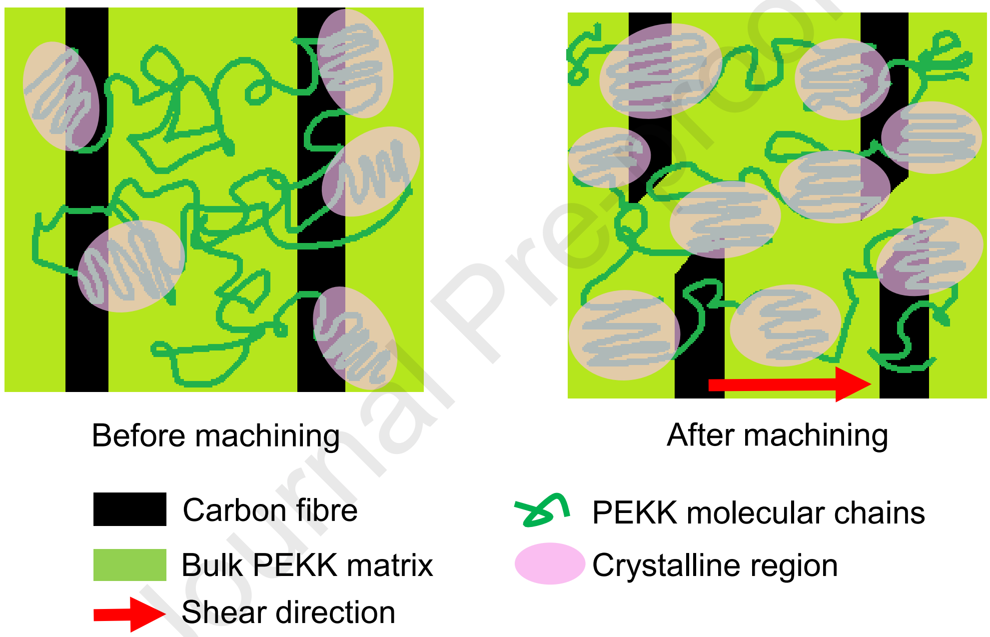

Fig. 12 Schematic diagram of strain induced crystallization in machined CF/PEKK chips

Compared to HM, CD exhibited greater crystallinity increase. This can be attributed to the greater cutting force and temperature experienced by the chip under CD. As the temperature approaches T_g, the PEKK matrix will experience the transition from glass to rubber-like state, the better flow and sliding of the molecular chains can further facilitate the re-alignment of the polymer molecules and increase crystallinity.

3.6. Material removal mechanism

For easier microstructural inspection and interpretation of the underlying material removal mechanism, the analysis was focused on CD chips and hole wall with 0° and 90° fibre orientation. As depicted in Fig. 13 and Fig. 14, for both fibre orientations, the material removal involves combined brittle fibre fracture and plastic deformation of the PEKK matrix. The cutting process can be explained by the

Ernst and Merchant's shear cutting model [64], where the shear plane assumption is applied to interpret the formation of continuous chips formed by the CF/PEKK composite.

As shown in Fig. 13 (a), for 0° fibre orientation, the cutting edge exerts a compressive stress to the workpiece along the fibre direction and an in-plane shear stress is generated along the fibre-matrix interface [53]. With the advancement of the tool, the removed carbon fibre will be subjected to extensive bending against the tool rake face. Brittle fibre fracture occurs when the external stress exceeds the bending strength limit of carbon fibre. Despite the segmented fibres within, the chip remains an overall intact morphology, as the ductile PEKK matrix can sustain a significant amount of plastic deformation, holding the fractured fibres in place, see Fig. 13 (b). On the machined hole surface, the high machining temperature can soften the matrix, and the highly viscous matrix can be re-casted and smeared at certain regions of hole surface (see Fig. 13 (c, d)). The evident fibre breakage on the machined hole surface is a result of the compressive action exerted by the tool cutting edge and rake face in the workpiece thickness direction.

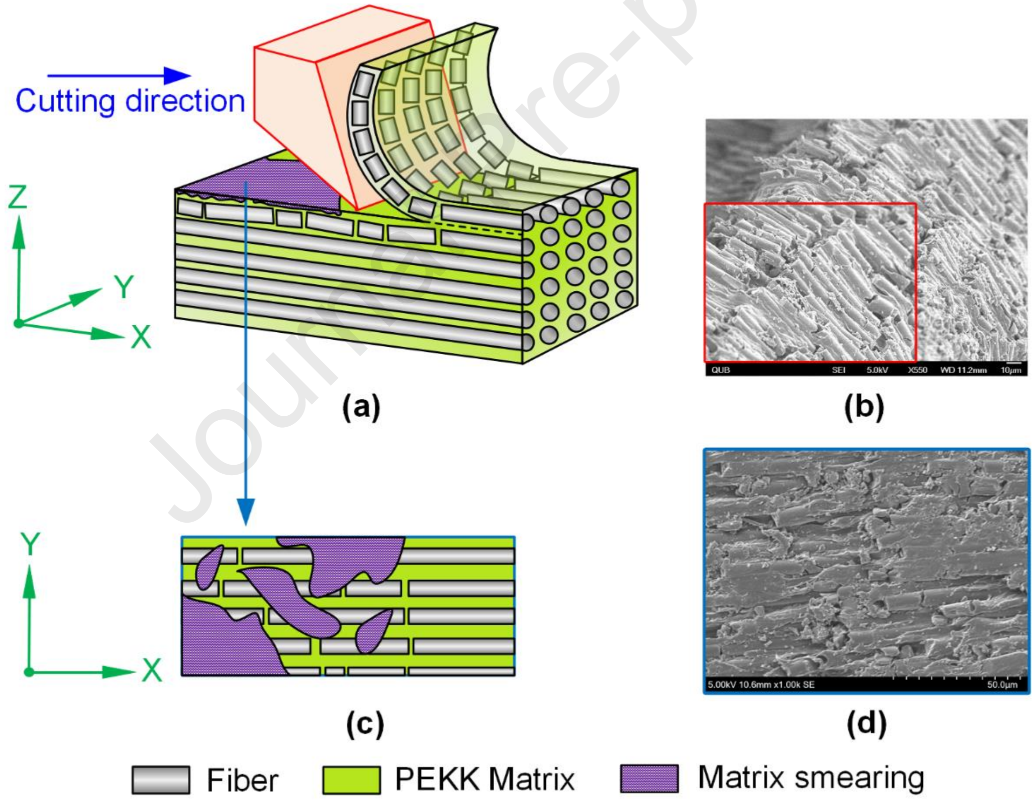

Fig. 13 (a) Schematic diagram of chip formation of CF/PEKK (0° fibre orientation), (b) Close-up SEM image of chip surface (0° fibre orientation) showing fractured fibres, (c) Top view schematic of the machined hole wall and (d) Close-up SEM image showing matrix smearing and fractured fibres on machined hole wall.

For 90° fibre orientation as illustrated by Fig. 14 (a), the cutting speed is perpendicular to the fibre direction. The carbon fibres undergo brittle fracture as a result of the shearing action of the cutting edge and the fracture plane is perpendicular to the fibre direction. Again, despite its plastic deformation, the highly ductile PEKK matrix has held the broken fibres in place, Fig. 14 (b). Similar matrix smearing was found on the hole surface. Bending-induced fibre debonding and fibre breakage have been found on the machined hole surface. Some of the broken fibres were found to be embedded in the smeared matrix on the machined hole surface, Fig. 14 (c, d).

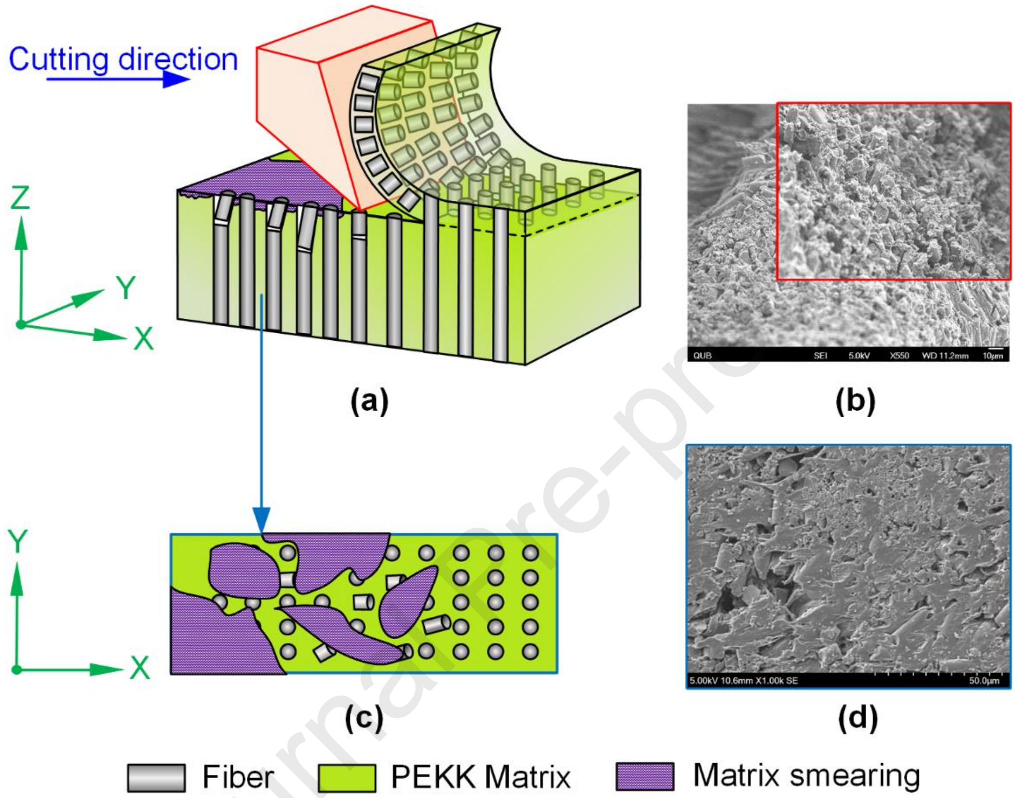

Fig. 14 (a) Schematic diagram of chip formation of CF/PEKK (90° fibre orientation), (b) Close-up SEM image of chip surface (90° fibre orientation) showing fractured fibres, (c) Top view schematic of the machined hole wall and (d) Close-up SEM image showing matrix smearing and fractured fibres on machined hole wall.

It is expected the unique material removal mechanism and the associated material structural change discovered in this study can be generalized to a wide of range of CFRTP materials, such as CF/PEEK, CF/PPS, CF/ABS, etc. Our preliminary work also inspires the research into orthogonal cutting of CFRTPs, through which more comprehensive understanding on the effect of cutting depth, cutting speed and temperature on the material removal mechanism can be elucidated. Although in-depth microstructural and thermal analysis has been carried out for chips in this study, measuring thermal property of the machined hole wall surface layer is not feasible with the current instrumentation. It is expected that the hole wall surface, particularly the smeared matrix, would have experienced similar shear induced crystallization. According to the literature, strain induced crystallization can potentially alter the stiffness, strength and fracture toughness of the material [62,65]. In the future, it will be valuable to investigate how machining induced structural/property variation would impact the mechanical performance of CFRTP components.

4. Conclusions

This paper reports the first investigation on hole making performance of thermoplastic CF/PEKK composite. Different hole making methods (CD and HM) and the effect of different feed rates on the resulting thrust force, machining temperature, delamination damage, hole microstructure and chip morphology/crystallinity have been investigated in detail. The main conclusions and contributions are as follows:

- CD generates higher thrust force than HM. The CD thrust force and feed rate follow a quasi-linear increasing relationship, whereas the thrust force of HM is independent on its feed rate.
- The tool temperature for both CD and HM decreases with the feed rate. HM shows a much higher tool temperature than CD, and this can be attributed to its prolonged tool engagement time and the associated heat accumulation.
- The CF/PEKK delamination damage is a result of combined thermal-mechanical interaction. For CD under low feed rate, the high machining temperature plays a more predominant role whereas under higher feed rate (lower temperature), the high thrust force would be more dominating. For HM, the delamination damage formation is mainly influenced by the high machining temperature, as the thrust force remains constant within the range of feed rate being investigated.
- Matrix smearing has been observed on both CD and HM hole walls. This is due to the softening and recasting of the highly ductile PEKK matrix onto the hole surface. Hole wall microstructural damages such as matrix loss and surface cavity are more severe for CD.
- CD leads to formation of continuous chips, which can be attributed to the continuous material removal process during drilling and the excellent ductility of the PEKK matrix. Under lower feed rate (< 0.05 mm/rev), the long and folded chips tend to clog the tools. Under higher feed rate (> 0.1 mm/rev), shorter, spiral shaped chips can be effectively evacuated. In contrast, HM produced short fragmented powdery chips as a result of the intermittent material removal process.
- Chips produced by both CD and HM show increased crystallinity as a result of shear induced crystallization, with CD (0.2 mm/rev) giving the greatest (300%) crystallinity enhancement.
- Through advanced material characterization, a greater insight has been developed into the machined CFRTP deformation characteristics, material removal mechanisms, and the associated material structural evolution at microscopic and molecular levels. These findings would inspire future researchers to better deploy the material process - structure - property relationship for optimized CFRTP manufacturing.

CRediT authorship contribution statement

Jia Ge: Conceptualization**,** Methodology, Investigation, Writing - Original Draft **Giuseppe Catalanotti:** Supervision, Writing - Review & Editing **Brian Falzon:** Writing - Review & Editing **John McClelland:** Software, Resources, Writing - Review & Editing **Colm Higgins:** Resources, Writing - Review & Editing **Yan Jin:** Supervision, Writing - Review & Editing, Funding acquisition, Project administration **Dan Sun:** Conceptualization, Methodology, Investigation, Writing - Review & Editing, Funding acquisition, Project administration.

Declaration of competing interest

The authors declare that they have no known competing financial interests or personal relationships that could have appeared to influence the work reported in this paper.

Acknowledgements

The funding support from EPSRC projects EP/P025447/1 and EP/P026087/1 is acknowledged. This project has also received funding from the European Union's Horizon 2020 research and innovation programme under grant agreement No 734272.

Appendix A

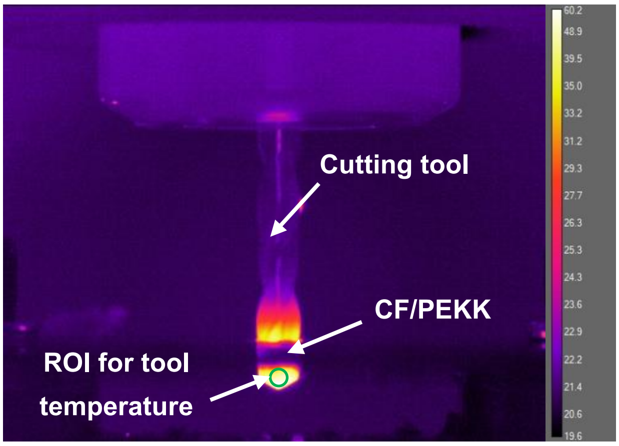

Fig. A.1 Tool temperature measurement at the hole exit (CD with feed rate F=0.2mm/rev)

Appendix B

Table B.1 Tool engagement time of CD and HM under different feed rates

Feed rate (mm/rev)	Method	
	CD	HM
0.025	4.4 s	77.7 s
0.05	2.2 s	37.8 s
0.1	1.1 s	18.7 s
0.15	0.7 s	12.4 s
0.2	0.5 s	9.3 s

Appendix C

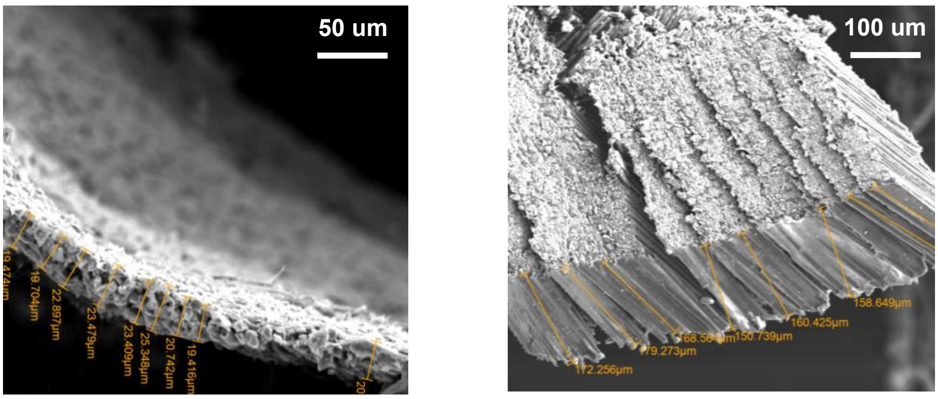

(a) CD F=0.025 mm/rev (b) CD F=0.2 mm/rev

Fig. C. 1 Thickness measurement of chips produced by CD under different feed rates

References

[1] R. Stewart, Thermoplastic composites — recyclable and fast to process, Reinf. Plast. 55 (2011) 22–28. https://doi.org/https://doi.org/10.1016/S0034-3617(11)70073-X.

[2] R. Stewart, Thermoplastic composites — recyclable and fast to process, Reinf. Plast. 55 (2011) 22–28. https://doi.org/https://doi.org/10.1016/S0034-3617(11)70073-X.

[3] R.L. Mazur, G.M. Cândido, M.C. Rezende, E.C. Botelho, Accelerated aging effects on carbon fiber PEKK composites manufactured by hot compression molding, J. Thermoplast. Compos. Mater. 29 (2016) 1429–1442. https://doi.org/10.1177/0892705714564283.

[4] Solvay, APC (PEKK) Thermoplastic composite tapes, (n.d.). https://www.solvay.com/en/product/apc-pekk-thermoplastic-composite-tapes.

[5] Thermoplastic composites gain leading edge on the A380, (n.d.). https://www.compositesworld.com/articles/thermoplastic-composites-gain-leading-edge-on-the-a380.

[6] New thermoplastic composite design concepts and their automated manufacture, (n.d.). https://www.jeccomposites.com/news/new-thermoplastic-composite-design-concepts-and-their-automated-manufacture/.

[7] Thermoplastic Upper Spar for an Aircraft Engine Pylon, (n.d.). https://www.toraytac.com/media/story/HelI/Thermoplastic-Upper-Spar-for-an-Aircraft-Engine-Pylon.

[8] Thermoplastic composite demonstrators — EU roadmap for future airframes, (n.d.). https://www.compositesworld.com/articles/thermoplastic-composite-demonstrators-eu-roadmap-for-future-airframes-.

[9] A. Yousefpour, M. Hojjati, J.P. Immarigeon, Fusion bonding/welding of thermoplastic composites, J. Thermoplast. Compos. Mater. 17 (2004) 303–341. https://doi.org/10.1177/0892705704045187.

[10] D. Meinhard, A. Haeger, V. Knoblauch, Drilling induced defects on carbon fiber-reinforced thermoplastic polyamide and their effect on mechanical properties, Compos. Struct. 256 (2021) 113138. https://doi.org/10.1016/j.compstruct.2020.113138.

[11] G.-D. Wang, S.K. Melly, N. Li, T. Peng, Y. Li, Research on milling strategies to reduce delamination damage during machining of holes in CFRP/Ti stack, Compos. Struct. 200 (2018) 679–688. https://doi.org/https://doi.org/10.1016/j.compstruct.2018.06.011.

[12] D. Sun, P. Lemoine, D. Keys, P. Doyle, S. Malinov, Q. Zhao, X. Qin, Y. Jin, Hole-making processes and their impacts on the microstructure and fatigue response of aircraft alloys, Int. J. Adv. Manuf. Technol. 94 (2018) 1719–1726. https://doi.org/10.1007/s00170-016-9850-3.

[13] R.B.D. Pereira, L.C. Brandão, A.P. de Paiva, J.R. Ferreira, J.P. Davim, A review of helical milling process, Int. J. Mach. Tools Manuf. 120 (2017) 27–48. https://doi.org/10.1016/j.ijmachtools.2017.05.002.

[14] V. Krishnaraj, A. Prabukarthi, A. Ramanathan, N. Elanghovan, M.S. Kumar, R. Zitoune, J.P. Davim, Optimization of machining parameters at high speed drilling of carbon fiber reinforced plastic (CFRP) laminates, Compos. Part B Eng. 43 (2012) 1791–1799. https://doi.org/10.1016/j.compositesb.2012.01.007.

[15] R.Q. Sardiñas, P. Reis, J.P. Davim, Multi-objective optimization of cutting parameters for

drilling laminate composite materials by using genetic algorithms, Compos. Sci. Technol. 66 (2006) 3083–3088. https://doi.org/10.1016/j.compscitech.2006.05.003.

[16] Q. Wang, X. Jia, Multi-objective optimization of CFRP drilling parameters with a hybrid method integrating the ANN, NSGA-II and fuzzy C-means, Compos. Struct. 235 (2020) 111803. https://doi.org/https://doi.org/10.1016/j.compstruct.2019.111803.

[17] N. Feito, A. Muñoz-Sánchez, A. Díaz-Álvarez, M.H. Miguelez, Multi-objective optimization analysis of cutting parameters when drilling composite materials with special geometry drills, Compos. Struct. 225 (2019) 111187. https://doi.org/10.1016/j.compstruct.2019.111187.

[18] N. Geier, J.P. Davim, T. Szalay, Advanced cutting tools and technologies for drilling carbon fibre reinforced polymer (CFRP) composites: A review, Compos. Part A Appl. Sci. Manuf. 125 (2019). https://doi.org/10.1016/j.compositesa.2019.105552.

[19] D.M. Guo, Q. Wen, H. Gao, Y.J. Bao, Prediction of the cutting forces generated in the drilling of carbon-fibre-reinforced plastic composites using a twist drill, Proc. Inst. Mech. Eng. Part B J. Eng. Manuf. 226 (2012) 28–42. https://doi.org/10.1177/0954405411419128.

[20] A. Langella, L. Nele, A. Maio, A torque and thrust prediction model for drilling of composite materials, Compos. Part A Appl. Sci. Manuf. 36 (2005) 83–93. https://doi.org/10.1016/j.compositesa.2004.06.024.

[21] M. Lazar, P.C. Xirouchakis, Mechanical load distribution along the main cutting edges in drilling, J. Mater. Process. Technol. 213 (2013) 245–260.

[22] Z. Qi, K. Zhang, H. Cheng, S. Liu, Numerical simulation for delamination during drilling of CFRP/AL stacks, Mater. Res. Innov. 19 (2015) S698–S6101. https://doi.org/10.1179/1432891715Z.0000000001457.

[23] Z. Jia, C. Chen, F. Wang, C. Zhang, Analytical study of delamination damage and delamination-free drilling method of CFRP composite, J. Mater. Process. Tech. 282 (2020) 116665. https://doi.org/10.1016/j.jmatprotec.2020.116665.

[24] S. Jain, D.C.H. Yang, Effects of Feedrate and Chisel Edge on Delamination in Composites Drilling, J. Eng. Ind. 115 (1993) 398–405. https://doi.org/10.1115/1.2901782.

[25] D.F. Liu, Y.J. Tang, W.L. Cong, A review of mechanical drilling for composite laminates, Compos. Struct. 94 (2012) 1265–1279. https://doi.org/10.1016/j.compstruct.2011.11.024.

[26] D. Geng, Y. Liu, Z. Shao, Z. Lu, J. Cai, X. Li, X. Jiang, D. Zhang, Delamination formation, evaluation and suppression during drilling of composite laminates: A review, Compos. Struct. 216 (2019) 168–186. https://doi.org/https://doi.org/10.1016/j.compstruct.2019.02.099.

[27] H. Hocheng, H.Y. Puw, On drilling characteristics of fiber-reinforced thermoset and thermoplastics, Int. J. Mach. Tools Manuf. 32 (1992) 583–592. https://doi.org/10.1016/0890-6955(92)90047-K.

[28] H. Hocheng, H.Y. Pwu, K.C. Yao, Machinability Of Some Fiber-Reinforced Thermoset And Thermoplastics In Drilling, Mater. Manuf. Process. 8 (1993) 653–682. https://doi.org/10.1080/10426919308934872.

[29] J. Xu, X. Huang, M. Chen, J. Paulo Davim, Drilling characteristics of carbon/epoxy and carbon/polyimide composites, Mater. Manuf. Process. 00 (2020) 1–9. https://doi.org/10.1080/10426914.2020.1784935.

[30] J. Xu, X. Huang, J.P. Davim, M. Ji, M. Chen, On the machining behavior of carbon fiber

reinforced polyimide and PEEK thermoplastic composites, Polym. Compos. 41 (2020) 3649–3663. https://doi.org/10.1002/pc.25663.
[31] A. Lopez-Arraiza, I. Amenabar, A. Agirregomezkorta, M. Sarrionandia, J. Aurrekoetxea, Experimental analysis of drilling damage in carbon-fiber reinforced thermoplastic laminates manufactured by resin transfer molding, J. Compos. Mater. 46 (2012) 717–725. https://doi.org/10.1177/0021998311414218.
[32] W. Zhang, Y. Xu, X. Hui, W. Zhang, A multi-dwell temperature profile design for the cure of thick CFRP composite laminates, Int. J. Adv. Manuf. Technol. (2021). https://doi.org/10.1007/s00170-021-07765-1.
[33] T. Choupin, Mechanical performances of PEKK thermoplastic composites linked to their processing parameters, 2018.
[34] M. Ferreira Batista, I. Basso, F. de Assis Toti, A. Roger Rodrigues, J. Ricardo Tarpani, Cryogenic drilling of carbon fibre reinforced thermoplastic and thermoset polymers, Compos. Struct. 251 (2020) 112625. https://doi.org/10.1016/j.compstruct.2020.112625.
[35] D. Kim, M. Ramulu, X. Doan, Influence of consolidation process on the drilling performance and machinability of PIXA-M and PEEK thermoplastic composites, J. Thermoplast. Compos. Mater. 18 (2005) 195–217. https://doi.org/10.1177/0892705705044556.
[36] F. Ahmad, A. Manral, P.K. Bajpai, Machining of Thermoplastic Composites, Springer Singapore, 2019. https://doi.org/10.1007/978-981-13-6019-0_8.
[37] I. Shyha, S.L. Soo, D.K. Aspinwall, S. Bradley, S. Dawson, C.J. Pretorius, Drilling of titanium/CFRP/aluminium stacks, Key Eng. Mater. 447 448 (2010) 624–633. https://doi.org/10.4028/www.scientific.net/KEM.447-448.624.
[38] J. Xu, A. Mkaddem, M. El Mansori, Recent advances in drilling hybrid FRP/Ti composite: A state-of-the-art review, Compos. Struct. 135 (2016) 316–338. https://doi.org/10.1016/j.compstruct.2015.09.028.
[39] W.J.B. Grouve, F. Sacchetti, E.J. Vruggink, R. Akkerman, Simulating the induction heating of cross-ply C/PEKK laminates–sensitivity and effect of material variability, Adv. Compos. Mater. 00 (2020) 1–22. https://doi.org/10.1080/09243046.2020.1783078.
[40] W. Haiyan, Q. Xuda, L. Hao, R. Chengzu, Analysis of cutting forces in helical milling of carbon fiber-reinforced plastics, Proc. Inst. Mech. Eng. Part B J. Eng. Manuf. 227 (2013) 62–74. https://doi.org/10.1177/0954405412464328.
[41] W. Haiyan, Q. Xuda, A mechanistic model for cutting force in helical milling of carbon fiber-reinforced polymers, Int. J. Adv. Manuf. Technol. 82 (2016) 1485–1494. https://doi.org/10.1007/s00170-015-7460-0.
[42] R. Fu, Z. Jia, F. Wang, Y. Jin, D. Sun, L. Yang, D. Cheng, Drill-exit temperature characteristics in drilling of UD and MD CFRP composites based on infrared thermography, Int. J. Mach. Tools Manuf. 135 (2018) 24–37. https://doi.org/https://doi.org/10.1016/j.ijmachtools.2018.08.002.
[43] J.P. Davim, J.C. Rubio, A.M. Abrao, A novel approach based on digital image analysis to evaluate the delamination factor after drilling composite laminates, Compos. Sci. Technol. 67 (2007) 1939–1945. https://doi.org/https://doi.org/10.1016/j.compscitech.2006.10.009.
[44] T.H. Lee, F.Y.C. Boey, K.A. Khor, On the determination of polymer crystallinity for a thermoplastic PPS composite by thermal analysis, Compos. Sci. Technol. 53 (1995) 259–274.

https://doi.org/https://doi.org/10.1016/0266-3538(94)00070-0.
[45] L. Quiroga Cortés, N. Caussé, E. Dantras, A. Lonjon, C. Lacabanne, Morphology and dynamical mechanical properties of poly ether ketone ketone (PEKK) with meta phenyl links, J. Appl. Polym. Sci. 133 (2016). https://doi.org/10.1002/app.43396.
[46] D. Geng, Y. Liu, Z. Shao, Z. Lu, J. Cai, X. Li, X. Jiang, D. Zhang, Delamination formation, evaluation and suppression during drilling of composite laminates: A review, Compos. Struct. 216 (2019) 168–186. https://doi.org/https://doi.org/10.1016/j.compstruct.2019.02.099.
[47] K. Thirukkumaran, M. Menaka, C.K. Mukhopadhyay, B. Venkatraman, A Study on Temperature Rise, Tool Wear, and Surface Roughness During Drilling of Al–5%SiC Composite, Arab. J. Sci. Eng. 45 (2020) 5407–5419. https://doi.org/10.1007/s13369-020-04427-4.
[48] K. Thirukkumaran, M. Menaka, C.K. Mukhopadhyay, B. Venkatraman, A Study on Temperature Rise, Tool Wear, and Surface Roughness During Drilling of Al–5%SiC Composite, Arab. J. Sci. Eng. 45 (2020) 5407–5419. https://doi.org/10.1007/s13369-020-04427-4.
[49] R. Stone, K. Krishnamurthy, A neural network thrust force controller to minimize delamination during drilling of graphite-epoxy laminates, Int. J. Mach. Tools Manuf. 36 (1996) 985–1003. https://doi.org/https://doi.org/10.1016/0890-6955(96)00013-2.
[50] R. Voss, M. Henerichs, F. Kuster, Comparison of conventional drilling and orbital drilling in machining carbon fibre reinforced plastics (CFRP), CIRP Ann. - Manuf. Technol. 65 (2016) 137–140. https://doi.org/10.1016/j.cirp.2016.04.001.
[51] N. Geier, J.P. Davim, T. Szalay, Advanced cutting tools and technologies for drilling carbon fibre reinforced polymer (CFRP) composites: A review, Compos. Part A Appl. Sci. Manuf. 125 (2019) 105552. https://doi.org/10.1016/j.compositesa.2019.105552.
[52] L. Quiroga Cortés, N. Caussé, E. Dantras, A. Lonjon, C. Lacabanne, Morphology and dynamical mechanical properties of poly ether ketone ketone (PEKK) with meta phenyl links, J. Appl. Polym. Sci. 133 (2016). https://doi.org/https://doi.org/10.1002/app.43396.
[53] Q. An, C. Cai, X. Cai, M. Chen, Experimental investigation on the cutting mechanism and surface generation in orthogonal cutting of UD-CFRP laminates, Compos. Struct. 230 (2019) 111441. https://doi.org/10.1016/j.compstruct.2019.111441.
[54] F. Ke, J. Ni, D.A. Stephenson, Continuous chip formation in drilling, Int. J. Mach. Tools Manuf. 45 (2005) 1652–1658. https://doi.org/https://doi.org/10.1016/j.ijmachtools.2005.03.011.
[55] A. Barman, R. Adhikari, G. Bolar, Evaluation of conventional drilling and helical milling for processing of holes in titanium alloy Ti6Al4V, Mater. Today Proc. 28 (2020) 2295–2300. https://doi.org/10.1016/j.matpr.2020.04.573.
[56] A.Z. Sultan, S. Sharif, D. Kurniawan, Chip Formation When Drilling AISI 316L Stainless Steel using Carbide Twist Drill, Procedia Manuf. 2 (2015) 224–229. https://doi.org/https://doi.org/10.1016/j.promfg.2015.07.039.
[57] Z. Zhu, K. Guo, J. Sun, J. Li, Y. Liu, L. Chen, Y. Zheng, Evolution of 3D chip morphology and phase transformation in dry drilling Ti6Al4V alloys, J. Manuf. Process. 34 (2018) 531–539. https://doi.org/https://doi.org/10.1016/j.jmapro.2018.07.001.
[58] R. Hussein, A. Sadek, M.A. Elbestawi, M.H. Attia, Chip morphology and delamination characterization for vibration-assisted drilling of carbon fiber-reinforced polymer, J. Manuf. Mater. Process. 3 (2019). https://doi.org/10.3390/jmmp3010023.

[59] S.O. Ismail, H.N. Dhakal, I. Popov, J. Beaugrand, Analysis and impacts of chips formation on hole quality during fibre-reinforced plastic composites machining, Adv. Transdiscipl. Eng. 3 (2016) 143–148. https://doi.org/10.3233/978-1-61499-668-2-143.
[60] J. Ahmad, Introduction to Polymer Composites, in: Mach. Polym. Compos., Springer US, Boston, MA, 2009: pp. 1–35. https://doi.org/10.1007/978-0-387-68619-6_1.
[61] M.C. Chien, R.A. Weiss, Strain-induced crystallization behavior of poly(ether ether ketone) (PEEK), Polym. Eng. \& Sci. 28 (1988) 6–12. https://doi.org/https://doi.org/10.1002/pen.760280103.
[62] R.-C. Zhang, Z. Huang, Z. Huang, M. Zhong, D. Zang, A. Lu, Y. Lin, B. Millar, G. Garet, J. Turner, G. Menary, D. Ji, L. Song, Q. Zhang, J. Zhang, D. Sun, Uniaxially stretched polyethylene/boron nitride nanocomposite films with metal-like thermal conductivity, Compos. Sci. Technol. 196 (2020) 108154. https://doi.org/https://doi.org/10.1016/j.compscitech.2020.108154.
[63] B. Mayoral, G. Menary, P. Martin, G. Garrett, B. Millar, P. Douglas, N. Khanam, M.A. AlMaadeed, M. Ouederni, A. Hamilton, D. Sun, Characterizing Biaxially Stretched Polypropylene / Graphene Nanoplatelet Composites, Front. Mater. 8 (2021) 232. https://doi.org/10.3389/fmats.2021.687282.
[64] H. Ernst, M.E. Merchant, Chip formation, friction and high quality machined surfaces, Surf. Treat. Met. ASM. 29 (1941) 299–378.
[65] B. Mayoral, G. Menary, P. Martin, G. Garrett, B. Millar, P. Douglas, N. Khanam, M.A. AlMaadeed, M. Ouederni, A. Hamilton, D. Sun, Characterizing Biaxially Stretched Polypropylene / Graphene Nanoplatelet Composites, Front. Mater. 8 (2021) 232. https://doi.org/10.3389/fmats.2021.687282.

Highlights:

- Hole making performance of CF/PEKK is investigated for the first time.
- A comparative study on conventional drilling and helical milling is reported.
- The role of thermo-mechanical interaction is elucidated for CF/PEKK hole making.
- Chip morphology and the associated material removal mechanism are revealed.
- Shear-induced crystallization caused by hole making is reported for the first time.

Declaration of interests

The authors declare that they have no known competing financial interests or personal relationships that could have appeared to influence the work reported in this paper.